EXPERIMENTAL STUDY FOR EARLY DETECTION OF BEARING DEFECTS BY VIBRATION AND ACOUSTIC EMISSION

Salim Meziani[a], Djamal Zarour[a-b], Marc Thomas[b]

[1] Laboratoire de Mécanique, Université des Frères Mentouri, Constantine 1, Algérie.Salim.meziani@umc.edu.dz

[2]Department of Mechanical Engineering, École de Technologie Supérieure. 1100, Notre-Dame street West, Montreal, H3C 1K3, Quebec, Canada.

zarourd@yahoo.fr,marc.thomas@etsmtl.ca

Abstract:

This research presents a design of experiments for early detection of bearing defects. Two measurement techniques (vibration and acoustic emission) are compared by using the ANOVA analysis. The results show the relationship between some time indicators to the degradation stage of bearing. The experimental design was considering the influence of the shaft speed, loadand defect size as independent variables while the dependent variables brought on different time indicators. The objective of this study is to compare the effectiveness, consistency and reliability for bearing defect monitoring by using vibration and acoustic emission measurements. The results lead us to favor the application of vibration because it adapts better to the vast majority of situations, while the acoustic emission allows for the reliable detection of the fault but not for accurate tracking. In fact, acoustic emission is recommend in the case of low speeds less than 400 rev/min. A new indicator called TALAF is most relevant for monitoring the defect size with a contribution of 97.87% in vibration and only of 76.35% by acoustic emission. Finally, the effects of shaft speed and the radial load increases with the defect size.

Keywords: Defect descriptor / Bearing defect /acoustic emission / envelope analysis / vibrations / ANOVA / early detection / load / operating speed.

1 Introduction

Rolling element bearings are one of the most essential parts of rotating machinery. A machine could be seriously jeopardized if defects occur in the bearings during service. Early detection of the defects is therefore crucial for the prevention of damage or total failure of the machinery. Different methods are used for detection and diagnosis of bearing defects; they may be broadly classified as vibration, acoustic analysis, temperature measurements, and wear debris analysis [1]. Among these, vibration analysis is the most widely used technique. Vibration signature based diagnostics are mainly concerned with the extraction of features from the vibratory signal, which can be related to a good or a defective state of the component [2]. Various signal processing techniques involving time, frequency, and statistical methods have been used to detect and check the progress of the incipient fault [3]. The extraction of meaningful information from these data is always challenging especially due to the presence of noise that masks the interesting information and, therefore, it calls for different approaches to analyze the data. A pertinent review of vibration measurement methods for the detection of defects in rolling element bearings is presented by Tandon and Chandhury[4]. The monitoring methods applied to bearings can be achieved in a number of ways, some of them being simple to use while others requiring sophisticated signal processing [5]. Shocks are usually created in the presence of faults and can be analyzed either in the time domain [6] (RMS and max-peak amplitude of vibration level, Crest factor and Kurtosis, detection of shock waves method [7], statistical parameters applied to the time signal, Cepstrum [8], etc.); or in the frequency domain (spectral analysis around bearing defect frequencies [9], Spike energy [10], high frequency demodulation [11], Empirical modal decomposition [12], acoustic emission [13], cyclostationnarity [14], time-frequency [15, 16], Fast Fourier Transform [17], Wavelet [18], Kurtogram [19], artificial neural networks [20], etc). Successful experimentation requires knowledge of important factors that may influence the output. A design of experiments (DOE)[21] helps to statistically understand the effect of various parameters on the investigated factor and determine the factors which are more significant for explaining a process variation. Furthermore, DOE allows for investigating the various interactions between the independent variables especially when proper understanding of the process may be difficult or impossible. Methods such as factorial design, response surface method (RSM), and Taguchi techniques may be used for planning the experiments.

The present work explores the application of Analysis of Variance (ANOVA) method using time domain features of the bearing vibrations and acoustic emission measurements as dependent variables for analyzing the effect of defect size, centrifugal load, and shaft speed on the bearing vibration. Time domain features such as RMS, crest factor, and kurtosis are generally used for statistical analysis. For the present study, the RMS, Peak, Crest, Kurtosis, k-factor, Skewness, TALAF and THIKAT of the signal has been used as the responses parameters [6]. TALAF and Skewness are considered to be good parameters to measure defectiveness in the bearings but irregularity in variation of Skewness makes it difficult for judging. Hence, the experiments were planned and analyzed using **ANOVA** approach to study the influence of the operating conditions on responses parameters. The experiments are performed on bearings having a defect on outer race.

2 Materials and methods

Experimental tests were carried out on the test bench Dynamo laboratory of ÉTS. The test bench is composed of a shaft driven by an electric motor (Fig.1-A), with speed controlled by a drive controller. The shaft is guided in rotation by two bearings and connected to the motor by a flanged coupling bolted rubber. At the end of this shaft is located a disc weight of 4.7 kg, which can be loaded with unbalance mass (which provides a rotating load and thus a centrifugal force).

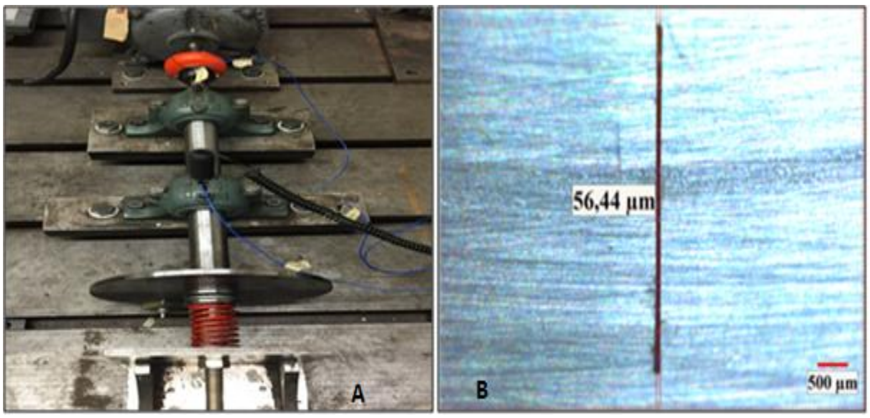

Figure 1. (A) Experimental setup, (B) A very small defect of outer race.

The bearings used are "ball bearings, cylindrical and tapered bore" SKF brand and 1210 EKTN9 model. The bearings have induced defects (groove) of different sizes on the outer race. Since the objective of this study is the early detection of defects, grooves with very small width were artificially created by electro-erosion and measured with a microscope. Two healthy bearings and three defective bearings with groove widths of 50, 100 and 150 micrometers were used. The frequencies [1] symptomatic of the defect of the bearings are shown in (Tab. 1). Since the defect is located on the outer race, the amplitude of Ball Pass Outer Race (BPFO) frequency is expected to increase with the defect size.

Table 1. Bearing frequencies 1210 EKTN9.

Rotation frequency	2xBSF	BPFO	BPFI
Order 1	Order 6.55	Order 7.24	Order 9.76

The acquisition chain is shown in "Figure 2". It is composed of two piezoelectric sensors (352C34) with a sensitivity of 100 mV/g, for the measurement of vibration, and an ultrasonic detector SystemsUltraProb EU 10000, for measuring the acoustic emission. The ultrasonic sensor operates in the lower ultrasonic spectrum from 20 kHz to 100 kHz. A heterodyne circuit converts the high frequency AE signal as detected by the transducer around a central frequency Fc into an audible signal (0-7 kHz) (Fig.2 - B). Both sensors are connected to an analogue digital converter THOR PRO Analyzer: DT9837-13310, with a sampling frequency of 48 kHz. Each recording lasted 5 seconds, which means that each time data file contains 240 000 samples. Using a tachometer was also necessary to verify that the actual speed of the shaft corresponds to that displayed on the inverter.

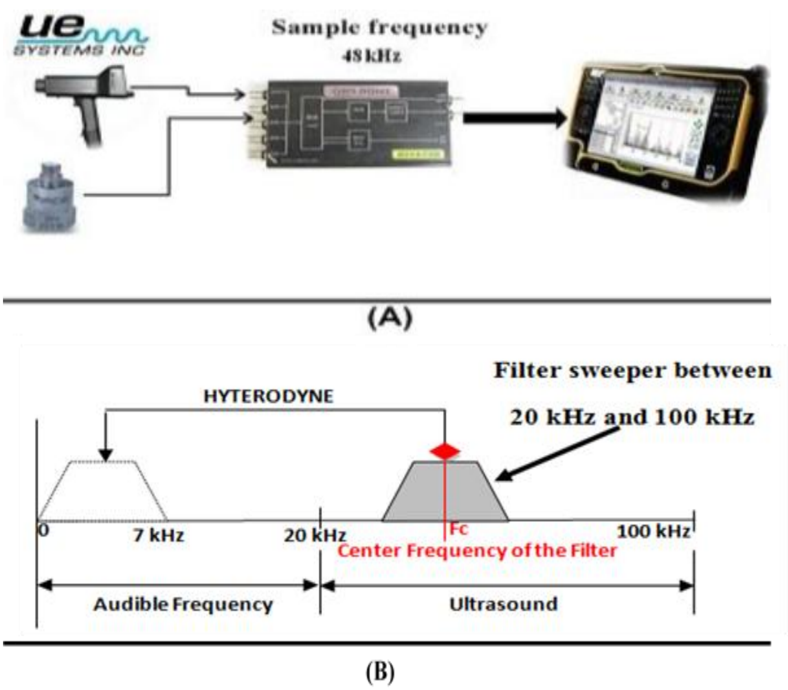

Figure 2. Data acquisition system.

2.1 The design of experiments

The considered factors are the default size (4 sizes), the radial load (3 loads) and shaft speed (5 speeds). All the tests were randomly duplicated three times in order to obtain the confidence interval. "Table 2" presents the factors and levels. The Statgraphics software was used to prepare the plan of experiments and analyze the results. A full factorial design was selected for accuracy and the experimental plan included all possible combinations. This means that it should take 3 × 4 × 5 × 3 = 180 trials.

Table 2. Summary of design of experiments

Shaft speed	Defect size	Centrifugal force	Number of tests
300 tr/min	0 µm	50 N	1
400 tr/min	50 µm	130 N	2
600 tr/min	100 µm	210 N	3
800 tr/min	150 µm		
900 tr/min			

Equation 1 was used to calculate the effect of the centrifugal load. Note that the speed and rotating load are dependent on each other. To study their effects separately a method based on the use of multiple masses for adjusting the rotational force effect was used.

$$f = m \times R \times \omega^2 \qquad (1)$$

The objective is to maintain 3 force levels for each speed, "Table 3" summarizes the 15 different masses to be applied to offset the effects of speed and keep the three load levels.

Table 3. Summary of compensation masses

Shaft speed (tr/min)	Shaft speed (rad/sec)	Centrifugal force (Newton)	applied mass (gram)
300 tr/min	31.42 rad/sec	50 N	441
		130 N	1145
		210 N	1850
400 tr/min	41.89 rad/sec	50 N	248
		130 N	644
		210 N	1041
600 tr/min	62.83 rad/sec	50 N	110
		130 N	286
		210 N	463
800 tr/min	83.77 rad/sec	50 N	62
		130 N	161
		210 N	260
900 tr/min	94.25 rad/sec	50 N	49
		130 N	127
		210 N	206

3 Results analysis

3.1 Time descriptors

In the time domain, the statistical descriptors considered as dependent variables were the RMS, Peak, Crest factor, Kurtosis, K-Factor, skewness, TALAF and THIKAT. They are detailed in "Table 4". These indicators were used to compare their effectiveness in the field of monitoring bearings at a stage of early degradation, using vibration and acoustic measurements.

Table 4. Time descriptors.

$R.M.S = \sqrt{\frac{1}{N}\sum_{i=1}^{N}(x_i - \bar{x})^2}$	$TALAF = log\left[Kurtosis + \frac{RMS}{RMS_0}\right]$
$Kurtosis = \frac{\frac{1}{N}\sum_{i=1}^{N}(x_i - \bar{x})^4}{R.M.S.^4}$	$THIKAT = log\left[Kurtosis^{crest\ factor} + \left(\frac{RMS}{RMS_0}\right)^{Peak}\right]$
$Crest\ factor\ = \frac{Peak}{R.M.S.}$	$K - Factor\ = Peak \times R.M.S$
$Peak = Sup_{1 \leq i \leq N}\lvert Xi \rvert$	$Skewness = \frac{1}{N}\sum_{i=1}^{N}\left(\frac{x_i - \bar{x}}{R.M.S}\right)^3$

3.2 Frequency indicator

In the frequency domain we chose the amplitude of the first peak BPFO (Ball Pass Outer Race) with its modulations because it is the only one able to locate the fault, even if it is slightly less sensitive. Taking account of its modulations relative to the rotational frequency can gain precision.

3.2.1 Statistical comparison of the time descriptors between vibration and acoustic emission

The results of the analysis of variance "ANOVA" for the different responses are given in the "Tables 5 and 6". The analysis is performed for a significance level α = 0.05 (confidence level of 95%). In these tables, the percentage contribution of each factor and their interactions is mentioned. Note that the TALAF indicator is strongly influenced by the defect size factor both in vibration and acoustic emission.

Table 5. Percentage contribution (%), F-ratio and P-value of different factors and interactions in vibrations.

		RMS	Kurtosis	Peak	C-Factor	K-Factor	Skewness	TALAF	THIKAT	BPFO
A	(%)	26,52	90,24	52,11	77,64	35,86	**95,99**	**97,87**	82,79	39,05
	F-ratio	3138,03	987,01	381,77	99,04	508,76	949,27	5045,26	181,12	1132,21
	P-value	0,00	0,00	0,00	0,00	0,00	0,00	0,00	0,00	0,00
B	(%)	69,65	6,56	43,38	13,16	55,45	2,56	1,44	11,00	55,36
	F-ratio	8242,46	71,72	317,81	16,79	786,73	25,27	74,07	24,07	1605,06
	P-value	0,00	0,00	0,00	0,00	0,00	0,00	0,00	0,00	0,00

C	(%)	0,27	0,85	0,14	0,90	0,75	0,01	0,15	0,88	0,15
	F-ratio	32,34	9,35	1,05	1,15	10,59	0,06	7,5	1,92	4,43
	P-value	0,00	0,00	0,35	0,32	0,00	0,95	0,00	0,15	0,01
D	(%)	0,02	0,09	0,00	0,02	0,02	0,04	0,01	0,02	0,00
	F-ratio	2,17	1,01	0,03	0,03	0,23	0,38	0,65	0,05	0,04
	P-value	0,12	0,37	0,97	0,97	0,79	0,69	0,52	0,95	0,96
AB	(%)	3,37	0,78	3,33	2,56	6,94	0,79	0,23	1,68	5,14
	F-ratio	399,22	8,56	24,39	3,26	98,54	7,82	11,98	3,67	149,14
	P-value	0,00	0,00	0,00	0,00	0,00	0,00	0,00	0,00	0,00
AC	(%)	0,04	0,41	0,26	2,16	0,26	0,19	0,09	1,25	0,11
	F-ratio	4,58	4,51	1,91	2,75	3,71	1,9	4,39	2,74	3,26
	P-value	0,00	0,00	0,08	0,02	0,00	0,09	0,00	0,02	0,01
AD	(%)	0,00	0,11	0,07	0,72	0,03	0,05	0,02	0,41	0,02
	F-ratio	0,59	1,25	0,52	0,92	0,47	0,54	0,9	0,9	0,46
	P-value	0,74	0,28	0,79	0,48	0,83	0,77	0,50	0,49	0,84
BC	(%)	0,11	0,70	0,57	1,69	0,65	0,20	0,16	1,28	0,14
	F-ratio	12,8	7,66	4,18	2,15	9,22	1,95	8,49	2,8	4,01
	P-value	0,00	0,00	0,00	0,04	0,00	0,06	0,00	0,01	0,00
BD	(%)	0,01	0,13	0,08	0,59	0,04	0,10	0,02	0,37	0,02
	F-ratio	0,95	1,37	0,56	0,75	0,54	0,94	0,9	0,81	0,54
	P-value	0,48	0,22	0,81	0,65	0,82	0,48	0,52	0,59	0,82
CD	(%)	0,00	0,13	0,05	0,57	0,01	0,08	0,02	0,32	0,01
	F-ratio	0,36	1,38	0,38	0,73	0,11	0,77	1,01	0,7	0,30
	P-value	0,84	0,25	0,83	0,57	0,98	0,55	0,41	0,59	0,88

As already mentioned, the number of tests has been considered as a factor. From the results shown in "Table 5", it is noted that the number of tests factor has no effect, which means that all the experiments are reliable.

It is also found that the effect of the centrifugal force is not large compared to other factors (rotation speed and defect size). Indeed, the radial loads are not sufficiently large to observe effects on vibration. This limit is due to the configuration of the test bench.

The speed and size of the defect have a fairly significant impact on the indicators. Indeed, an indicator such as the vibration TALAF, which is influenced 97.87% by defect, determines the size of the defect without the knowledge of other parameters. However, the Peak and RMS does not directly derive the default size, as they are heavily influenced by the speed of rotation. They thus require the additional knowledge of the speed of rotation in order to determine the size of the defect.

Table 6. Percentage contribution (%), F-ratio and P-value of different factors and interactions in acoustic emission

		RMS	Kurtosis	Peak	C-Factor	K-Factor	Skewness	TALAF	THIKAT	BPFO
A	(%)	7,93	31,68	32,85	49,20	18,75	59,71	76,35	47,5	27,16
	F-ratio	306,99	7,02	261,51	50,08	228,93	40,33	193,14	56,59	664,07
	P-value	0	0,0002	0	0	0	0	0	0	0,00

B	(%)	88,98	22,65	62,38	37,12	72,56	22,74	17,14	37,4	66,94
	F-ratio	3446,34	5,02	496,63	37,78	886,01	15,36	43,35	44,52	1636,74
	P-value	0	0,0009	0	0	0	0	0	0	0,00
C	(%)	0,53	7,27	1,07	0,03	2,15	1,29	0,11	0,34	0,08
	F-ratio	20,72	1,61	8,51	0,03	26,23	0,87	0,29	0,41	1,95
	P-value	0	0,2031	0,0003	0,9732	0	0,4215	0,7517	0,6635	0,15
D	(%)	0,02	5,19	0,08	2,53	0,01	2,49	0,57	2,93	0,00
	F-ratio	0,64	1,15	0,67	2,58	0,17	1,68	1,45	3,49	0,10
	P-value	0,5295	0,3188	0,5128	0,0802	0,8469	0,1897	0,2394	0,0335	0,90
AB	(%)	1,95	8,48	2,47	5,95	4,82	6,13	3,26	6,69	5,46
	F-ratio	75,62	1,88	19,63	6,06	58,8	4,14	8,24	7,97	133,62
	P-value	0	0,0434	0	0	0	0	0	0	0,00
AC	(%)	0,40	10,60	0,36	1,94	0,70	4,31	1,40	2,29	0,23
	F-ratio	15,5	2,35	2,89	1,97	8,55	2,91	3,55	2,73	5,57
	P-value	0	0,0352	0,0115	0,0751	0	0,0108	0,0028	0,0158	0,00
AD	(%)	0,02	5,73	0,17	1,57	0,12	1,39	0,57	0,92	0,06
	F-ratio	0,67	1,27	1,32	1,6	1,49	0,94	1,45	1,1	1,47
	P-value	0,6762	0,2782	0,2522	0,1535	0,1879	0,4696	0,2015	0,3681	0,87
BC	(%)	0,16	3,25	0,53	0,42	0,83	0,71	0,22	0,70	0,02
	F-ratio	6,14	0,72	4,21	0,43	10,14	0,48	0,55	0,83	0,48
	P-value	0	0,6693	0,0002	0,8994	0	0,8701	0,8136	0,5814	0,19
BD	(%)	0,01	4,29	0,07	1,05	0,03	1,14	0,37	1,22	0,04
	F-ratio	0,5	0,95	0,59	1,07	0,36	0,77	0,93	1,45	0,86
	P-value	0,8542	0,4782	0,7842	0,386	0,938	0,6301	0,4962	0,1828	0,56
CD	(%)	0,01	0,86	0,02	0,18	0,03	0,09	0,00	0,08	0,01
	F-ratio	0,26	0,19	0,17	0,18	0,37	0,06	0,01	0,09	0,29
	P-value	0,9049	0,9433	0,9518	0,9468	0,8329	0,9939	0,9999	0,9859	0,88

"Table 6" is the percentage contribution factors and their interaction on the TALAF acoustic emission. Based on these results, we note that the TALAF is most sensitive to changes in the default size, with a contribution of 76.35%. It is followed by Skewness, contributing de 59, 71% and crest factor, with a contribution of 49.20%.

3.2.2 Study TALAF indicator

The results of the analysis of variance "ANOVA" for TALAF vibration and acoustic emission are given respectively in the "Tables 7 and 8". In these tables are listed the values of degrees of freedom (DF), the sum of squared deviations (SC sq), the mean square (MS), F value, the probability (p-value.) and contribution percentage (Cont. %) of each factor and different interactions.

Table 7. Analysis of variance (ANOVA) for vibration TALAF

Source	*SC sq.*	*DF*	*MS*	*F-value*	*p-value*	Cont. %
A:Defect size	20,4306	3	6,81019	5045,26	**0,0000**	**97,87%**
B:Shaft speed	0,399912	4	0,0999779	74,07	**0,0000**	1,44%
C:Load	0,0202425	2	0,0101212	7,50	**0,0008**	0,15%

D:Number test	0,00175902	2	0,000879508	0,65	0,5230	0,01%
AB	0,194034	12	0,0161695	11,98	**0,0000**	0,23%
AC	0,0355812	6	0,0059302	4,39	**0,0005**	0,09%
AD	0,00727955	6	0,00121326	0,90	0,4981	0,02%
BC	0,0917027	8	0,0114628	8,49	**0,0000**	0,16%
BD	0,00967902	8	0,00120988	0,90	0,5219	0,02%
CD	0,00543058	4	0,00135765	1,01	0,4072	0,02%
Error	0,167378	124	0,00134982			
TOTAL	21,3636	179				

According to the results, we note that all factors have a significant effect on the response TALAF except the factor number of tests. This confirms that the duplication of testing was good. In addition, the "default size" factor is predominant with a contribution of 97.87%, followed by the factor "speed" with 1.44%% and then the factor "Radial", with a contribution of 0, 15%. Interactions A×B, A×C and B×C are significant on the TALAF response, while interactions A×D, B×D and C×D are insignificant. According to "Figure 3", it is clear that the increase of TALAF is directly related to the increase in size of the defect. However, it is noted that this indicator tends to decrease with increasing speed of rotation and the radial load. This is due to the defect size, which is much smaller than the diameter of the ball. Also, TALAF is relevant and reliable to distinguish healthy from the unhealthy state of working condition. The effect of the factor "speed" in Figure 3 (a) "is significant in terms of increase of the size of the defect.

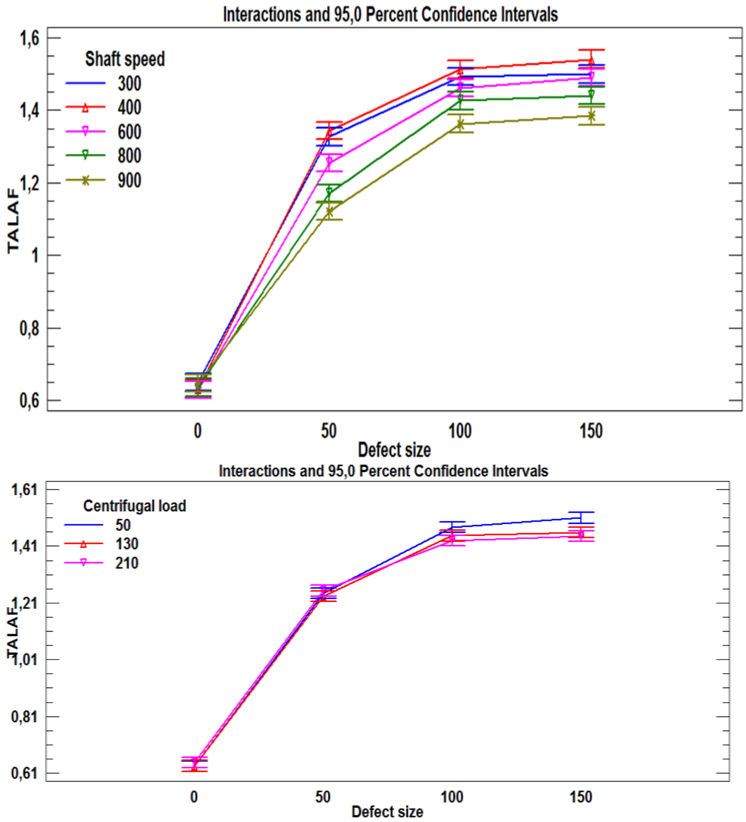

Figure 3. Curves of significant interactions for TALAF vibrations

The results of the analysis of variance "ANOVA" of TALAF able acoustic emission are shown in "Table 8". The contributions of factors "defect size" and "speed" are significant and are respectively of the order of 76.35% and 17.14%. On the contrary, the contributions of factors "Radial" and "number of tests" are non-significant. The interactions A×B and A×C are significant while the interaction A×D, B×C, B×D and C×D are not.

Table 8. Analysis of variance (ANOVA) for TALAF of acoustic emission

Source	*SC sq.*	*DF*	*MS*	*F-value*	*p-value*	Cont. %
A:Defect size	27,9754	3	9,32514	193,14	**0,0000**	76,35%
B:Shaft speed (rpm)	8,373	4	2,09325	43,35	**0,0000**	17,14%
C:Load(N)	0,0276252	2	0,0138126	0,29	0,7517	0,11%
D:Numbre test	0,139665	2	0,0698325	1,45	0,2394	0,57%
AB	4,77295	12	0,397746	8,24	**0,0000**	3,26%
AC	1,02709	6	0,171181	3,55	**0,0028**	1,40%
AD	0,419644	6	0,0699406	1,45	0,2015	0,57%
BC	0,21394	8	0,0267425	0,55	0,8136	0,22%
BD	0,358322	8	0,0447902	0,93	0,4962	0,37%
CD	0,00131741	4	0,000329353	0,01	0,9999	0,00%
Error	5,98704	124	0,0482826			
TOTAL	49,296	179				

In "Figure 4" is shown the significant interactions with TALAF. The results given in "Figure 4 (a)," show that the TALAF tends to increase with the increase of defect size and to decrease with increasing speed of rotation. The shape of the curve is consistent in low speed, in particular at the speed 400 rev / min or below.

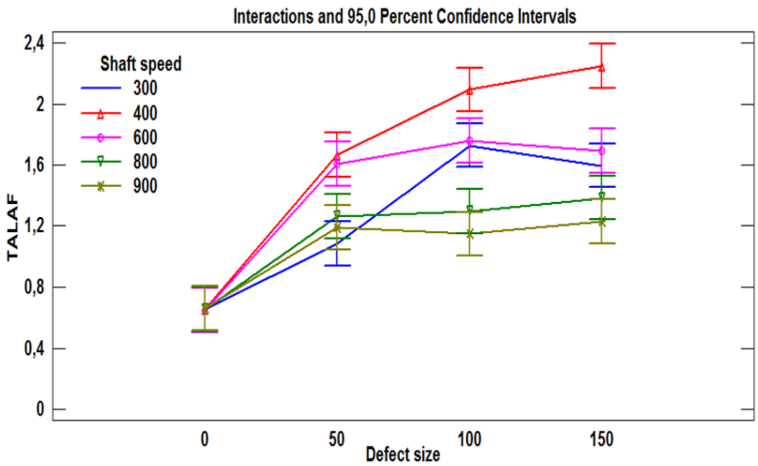

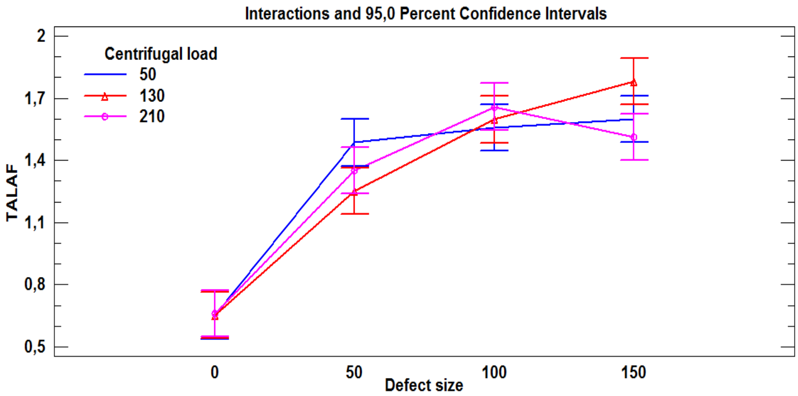

Figure 4. Curves of significant interactions for TALAF acoustic emission

4 Conclusion

The method of the analysis of variance "ANOVA" using a comprehensive plan of experiments demonstrated the ability to assess the influence of factors (speed, centrifugal load and size of the defect) on the vibration behavior and acoustics bearings an early stage of degradation. The comparative study of different time descriptors, showed the effectiveness of TALAF indicator for the detection and monitoring of the evolution of the size of the defects of the bearings with a contribution of 97.87% and 76.35 vibrations % by acoustic emission. Also, it was found that the effect of the speed of rotation and the radial load increases with increasing the size of the defects. The use of acoustic emission is efficient for the detection but not monitoring the evolution of the defect size.. It can be preferred especially in cases of low or very low speeds of less than 400 rev / min. Vibration measurement remains preferable to monitor the evolution of the defect size while the acoustic emission is more suited to the detection of frequencies characteristic of bearing defects at an early stage.

References

[1] M. Thomas, Fiabilité, maintenance prédictive et vibrations de machines: Presses de l'Université du Québec, 633 pages, D3357, ISBN 978-2-7605-3357-8, 2001.

[2] M.Thomas, Masounave J., Dao T.M., Le Dinh C.T. and Lafleur F, Rolling element bearing degradation and vibration signature relationship: 2nd international conference on monitoring and acoustical and vibratory diagnosis (SFM), Senlis, France, Vol.1, 1995, pp. 267-277.

[3] R.M.Jones, A guide to the interpretation of machinery vibration measurements, Sound and Vibration, Vol. 28, No 9, 1994, pp. 12-20.

[4] N.Tandon and A.Choudhury, A review of vibration and acoustic measurement methods for the detection of defects in rolling element bearings: Journal of Tribology International, 32, 1999, pp. 469-480.

[5] R.B. Randall and J. Antoni, Rolling element bearing diagnostics—A tutorial: Mechanical Systems and Signal Processing 25, 2011,pp. 485–520, 2011.

[6]S.Sassi, B.Badri and M. Thomas, Tracking surface degradation of ball bearings by means of new time domain scalar descriptors: International journal of COMADEM, 2008, ISSN1363-7681, 11 (3), pp. 36-45.

[7]B.Badri, M. Thomas and S.Sassi, The envelop Shock detector: a new method to detect impulsive signals, International journal of COMADEM. 15(3), 2012, pp.29-38.

[8]M.El Badaoui, Contribution of vibratory diagnostic of gearbox by Cepstral analysis: Ph.D. thesis, Jean Monnet University of St Etienne (FR), p. 141,1999 (in French).

[9]J.Berry, How to track rolling bearing health with vibration signature analysis: Sound and Vibration, 1991, pp. 24-35.

[10]J.C.M.De Priego, The relationship between vibration spectra and spike energy spectra for an electric motor bearing defect, Vibrations, Vol. 17, No 1, 2001, pp. 3-5.

[11]J. Altmann and J. Mathew, Multiple band-pass autoregressive demodulation for rolling-element bearing fault diagnosis: Mechanical Systems and Signal Processing 15 (5),2001, pp. 963–977.

[12]M. Kedadouche, M. Thomas and A. Tahan, Monitoring bearing defects by using a method combining EMD, MED and TKEO: Advances in Acoustics and Vibration. Hindawi Publishing Corporation, Vol 2014, ID 502080,10 p.,2014.

[13]M. Kedadouche, M. Thomas and A. Tahan. Cyclostationarity applied to acoustic emission and development of a new indicator for monitoring bearing defects: Mechanics & Industry, 5 (6),2014, pp. 467 – 476.

[14]J. Antoni, F. Bonnardot, A. Raada, M. El Badaoui, Cyclostationary modelling of rotating machine vibration signals, Mechanical Systems and Signal Processing, Volume 18, Issue 6, November 2004, pp. 1285–1314.

[15] M.S.Safizadeh, A.A.Lakis, and M.Thomas, Time-Frequency distributions and their Application to Machinery Fault Detection, International Journal of Condition Monitoring and Diagnosis Engineering Management, 5 (2), 2002, pp. 41-56.

[16] S.Braun, and M. Feldman,Time-Frequency Characteristics of Non-Linear Systems: Mechanical Systems and Signal Processing, 11(4), 1997,pp. 611-620.

[17] M.S.Safizadeh, A.A.Lakis,andM. Thomas, Using Short Time Fourier Transform in Machinery Fault Diagnosis: International Journal of Condition Monitoring and Diagnosis Engineering Management (COMADEM), 3 (1), 2000,pp 5-16.

[18] P. Tse, Y.H. Peng, R. Yam, Wavelet analysis and envelope detection for rolling element bearing fault diagnosis—their effectiveness and flexibility: Transactions of the ASME, Journal of Vibration and Acoustics 123 (3), 2001, pp. 303–310.

[19] J. Antoni, R.B. Randall,The spectral kurtosis: application to the vibratory surveillance and diagnostics of rotating machines: Mechanical Systems and Signal Processing, 20, 2006, pp. 308–331.

[20] L.Batista, B. Badri , R. Sabourin and M. Thomas, A Classifier Fusion System for Bearing Fault Diagnosis:Expert Systems with Applications, Elsevier, 40 (17), 2013, pp. 6788-6797.

[21] D. C.Montgomery, Design and Analysis of Experiments: 5th ed., Wiley, Singapore, 2007, pp. 21–46.